Hindawi
International Journal of Optics
Volume 2019, Article ID 8724320, 9 pages
https://doi.org/10.1155/2019/8724320

Research Article

Highly Fluorescent Nitrogen-Doped Graphene Quantum Dots' Synthesis and Their Applications as Fe(III) Ions Sensor

Fei Lu,[1] Yi-hua Zhou,[1] Li-hui Wu,[1] Jun Qian,[1] Sheng Cao,[2] Ya-feng Deng,[1] and Yuan Chen[1]

[1] *School of Printing and Packaging, Wuhan University, Wuhan 430079, Hubei, China*
[2] *Wuhan Donghu University, Wuhan 430079, Hubei, China*

Correspondence should be addressed to Yi-hua Zhou; yihuazhou@whu.edu.cn

Received 30 November 2018; Revised 4 February 2019; Accepted 26 February 2019; Published 1 April 2019

Academic Editor: Wonho Jhe

Nitrogen-doped graphene quantum dots (N-GQDs) with strong blue fluorescence and a high quantum yield of 88.9% were synthesized via a facile one-pot hydrothermal treatment with citric acid (CA) and ethylenediamine (EDA) as carbon and nitrogen sources, respectively. The blue fluorescence emission is independent of the excitation wavelengths. These N-GQDs dispersed well in water and ethyl alcohol and showed a highly selective and sensitive detection of hazardous and toxic Fe^{3+} in the range of 1600μmol/L to 6000μmol/L through a fluorescence quenching process with a detection limit of 2.37μmol/L. Based on the excellent sensitivity and selectivity of N-GQDs to heavy metal ions, paper-based sensors can be fabricated by inkjet printing, which are rapid but low cost. So the visual instant on-site identification of heavy metal ion will be realized in the future.

1. Introduction

Graphene quantum dots (GQDs) are carbon nanoparticles with a diameter less than 10 nm and luminescent properties [1, 2]. It has low preparation cost, good optical stability, low toxicity, good biocompatibility, and unique electronic properties [3–6]. It can be used as an electron acceptor or donor. It has good research and application value in cell imaging [7, 8], optoelectronic devices [9, 10], biological transmission [11], fluorescence anticounterfeiting [12, 13], and analysis and detection [14–19]. Nitrogen-doped graphene quantum dots (N-GQDs) have high quantum yield and excellent bleaching resistance of fluorescent materials [20, 21]. N-GQDs are widely used in new fluorescent sensors to detect metal ions [22–25], nonmetal ions [26], organic small molecules [27], and biological macromolecules [28].

The experiment of fluorescence sensor is simple and does not require complex pretreatment [29], but the quantitative and semiquantitative analysis of target still needs the help of fine fluorescence instruments, such as fluorescence spectrometer or confocal microscope [29]. Therefore, it is of great significance to develop a fast, sensitive, low cost, and portable visual testing equipment. The mechanism of detection of Fe3+ by adding N-GQDs should be further discussed [30–32].

In this paper, N-GQDs with a quantum yield (QY) of 88.9% and blue light were prepared by one-step hydrothermal method using citric acid as carbon source and ethylene diamine as nitrogen source. The syntheses were characterized by TEM, FT-IR, PL, and UV-Vis to explore the characteristics of N-GQDs. As shown in Figure 1, the prepared N-GQDs were used as high-efficiency fluorescent probes to detect iron ions qualitatively and quantitatively. A portable, miniature, and visualized fluorescent paper-based sensor was designed by fixing the carbon probe solution on the paper medium. For the occasions requiring on-site timely detection, especially for resource-poor countries and remote areas, test paper detection technology is very important, so the establishment of solid-phase fluorescence detection system has great research value and a bright prospect in exploitation system have in this paper.

2. Experiment

2.1. Materials and Experimental Instruments. The materials used are citric acid (CA), ethylene diamine (EDA),

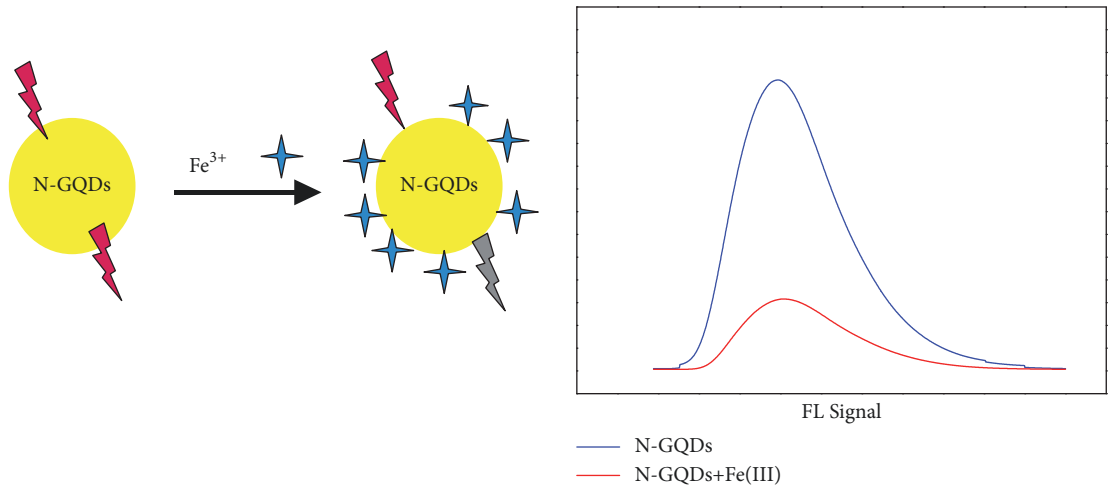

Figure 1: Fluorescence quenching of N-GQDs by iron ions.

alcohol, deionized water, phosphate buffer saline, and bond paper.

The instruments used are DZF-6020 Vacuum Dryer (Shanghai Xinmiao Co., Ltd.), AL-204-IC Electronic Analysis Balance (METTLER-TOLEDO), HP Printer 2050 (China Hewlett-Packard Co., Ltd.), KQ-300DE Ultrasound Cleaner (Kunshan Instrument Co., Ltd.), H1650-W Centrifuge (Xiangyi Co., Ltd.), FP-6500 Fluorescence Spectrometer (Jiashike (Part I) Hai) Trading Co., Ltd., UV-3600 Ultraviolet-Visible Spectrometer (Shimadzu Instruments and Equipment Co., Ltd.), TEM-2100 Transmission Electron Microscope (Japan Electronics Company), and FT-IR-5700 (Thermo Company, USA).

2.2. Preparation of N-GQDs. According to the molar ratio of 1:3, 0.21g (1 mmol) CA and 0.18g (3mmol) EDA were dissolved in 5mL distilled water by mechanical stirring to clear and transparent solution. The solution was transferred to 20mL reaction kettle and placed in oven. The temperature was programmed to 160°C for 4h. The product was washed with a large amount of ethanol and centrifuged for 5000rpm for 5 minutes. After separation and purification, 24h was frozen and dried.

2.3. Inkjet Based Paper Sensor. In this paper, a fluorescence quenching sensor for Fe^{3+} visualization detection was studied, and a quenching paper-based sensor was fabricated by inkjet printing technology. The fluorescent paper sensors were made by HP inkjet printer 2050. The ink in the cartridge was cleaned. The self-made N-GQDs probe solution was used as inkjet ink and injected into the empty cartridge. After online inkjet printing, start the predesigned pattern on the computer. The paper-based sensor with the best fluorescence intensity was obtained by exploring the composition of ink solution, ink concentration, and printing times. The printed patterns were observed and photographed under 365nm ultraviolet lamp, and the fluorescence intensity of the paper was scanned by fluorescence spectrometer.

2.4. Detection of Fe^{3+}

2.4.1. Detection of Fe^{3+} in Solvents. The 50mmol/L Fe^{3+} solution was diluted to 0-50mmol/L samples in turn. The prepared 2g/LN-GQDs solution was diluted to neutral solution with PBS buffer, and its 1mL was taken as standard solution of fluorescence probe. Then, a certain volume of Fe^{3+} with different concentrations was added to the solution, and its fluorescence spectrum was measured at a constant volume of 5mL.

2.4.2. Fe^{3+} Detection on Paper-Based Sensors. The quenching effect was observed at 365nm ultraviolet lamp by using a microinjector to extract a certain amount of iron ion solution with different concentrations and dropping it on a paper-based sensor. The concentration of Fe^{3+} is 0mmol/L, 0.05 mmol/L, 0.15mmol/L, 0.25mmol/L, 0.3mmol/L, 0.5mmol/L, 0.6mmol/L, 1.0mmol/L, and 2.0mmol/L in turn.

2.4.3. Selectivity of N-GQDs Fluorescent Probe to Fe^{3+}. In order to test the specificity of the fluorescent probe solution for Fe^{3+} detection, 1mL, 10 mmol/L Fe^{3+}, and other common metal ions (Cu^{2+}, Ag^{+}, Co^{2+}, Ba^{2+}, Al^{3+}, Mn^{2+}, Fe^{2+}, K^{+}, Na^{+}, and Zn^{2+}) were added into the N-GQDs solution. After 30 minutes of reaction, the fluorescence intensity of the probe solution was scanned to study the interaction between N-GQDs and other metal ions. Aiming at the selectivity of fluorescence quenching paper-based sensor, metal ions with the same concentration above 0.5mL were dripped on the paper-based sensor, waiting for paper-based drying, observing the experimental results under ultraviolet lamp, and investigating the interference experiment.

3. Results and Discussion

3.1. Optimum Preparation Conditions of N-GQDs

3.1.1. Morphology and Chemical Composition of N-GQDs. It can be seen from Figure 2 that N-GQDs is a spherical

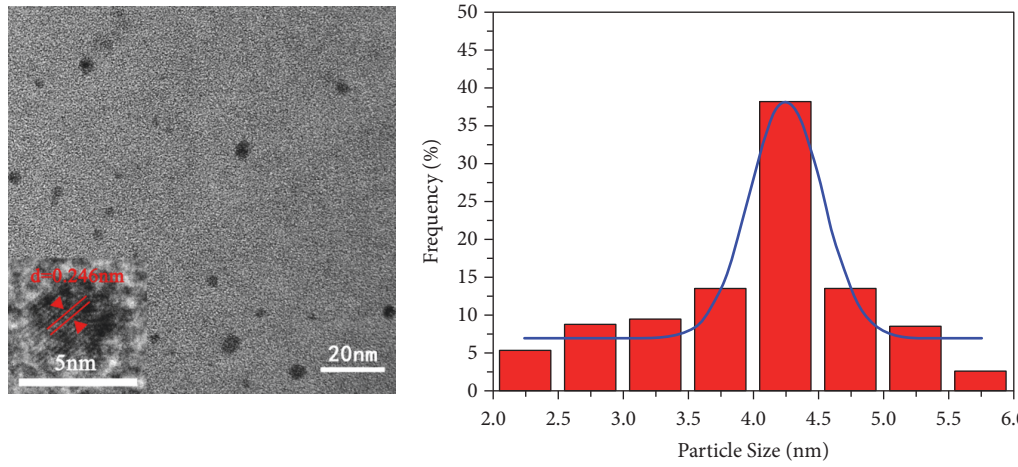

Figure 2: (a) TEM diagram of N-GQDs; (b) the size of distribution of the N-GQDs.

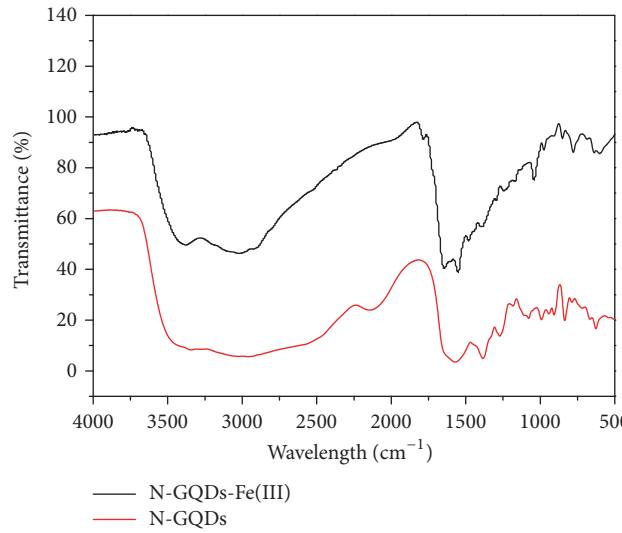

Figure 3: FT-IR diagrams of N-GQDs prepared by citric acid: ethylenediamine=1:3 and N-GQDs-Fe^{3+}.

shape; the average size is less than 4.05nm and disperses uniformly in aqueous solution, without agglomeration. The typical lattice spacing is 0.290nm, which shows a graphitic structure of the as-obtained N-GQDs [33].

As shown in Figure 3, 3436cm^{-1} shows the stretching vibration of -C-H bond, indicating that carbon quantum dots contain saturated alkyl groups, 3342cm^{-1} shows the stretching vibration of -OH bond, the strong peak at 3010cm^{-1} can vibrate of - NH_2 bond, 1562cm^{-1} can deduce the stretching vibration of -C=O-NH (peptide) bond, and 1396/1072cm^{-1} is the stretching vibration of -C-O bond. The stretching vibration peak at 1265cm^{-1} is the stretching vibration peak of C-O bond [34, 35]. Compared with the position of the characteristic peak of standard infrared spectrum, the characteristic peaks of N-H bond and C=O bond in the FT-IR spectrum belong to the amide bond characteristic peak, which indicates that the carbon quantum dots prepared in this study contain amide bond.

As is shown in Figure 3, black solid line, when Fe^{3+} bonds to the carbon quantum dots, the peak at 1820 cm^{-1} splits into two weak peaks, at 1830 and 1770cm^{-1}, respectively, while the peak at 1704 cm^{-1} weakens. This indicates that Fe^{3+} bonds to —COOH.

Figure 4 shows the typical peaks at 284.9eV, 286.5eV, and 288.2eV in the deconvoluted C1s XPS spectrum (Figure 4(b)) are attributed to the graphitic (C[double bond, length as m-dash]C and C—C), C—O, and C[double bond, length as m-dash]O, respectively. The typical peaks at 400.4eV in the N1s XPS spectrum (Figure 4(c)) reveal three different types of nitrides: pyridinic type, pyrrolic type, and N – H. The XPS analysis is consistent with the above FT-IR results [36].

Table 1 shows that carbon quantum dots are composed of four elements, C, N, H, and O, and contain saturated alkyl groups, amide bonds, and other functional groups. According to the elemental analysis table, under the condition of CA:EDA=1:3 (molar ratio), quantum dots contain more C,

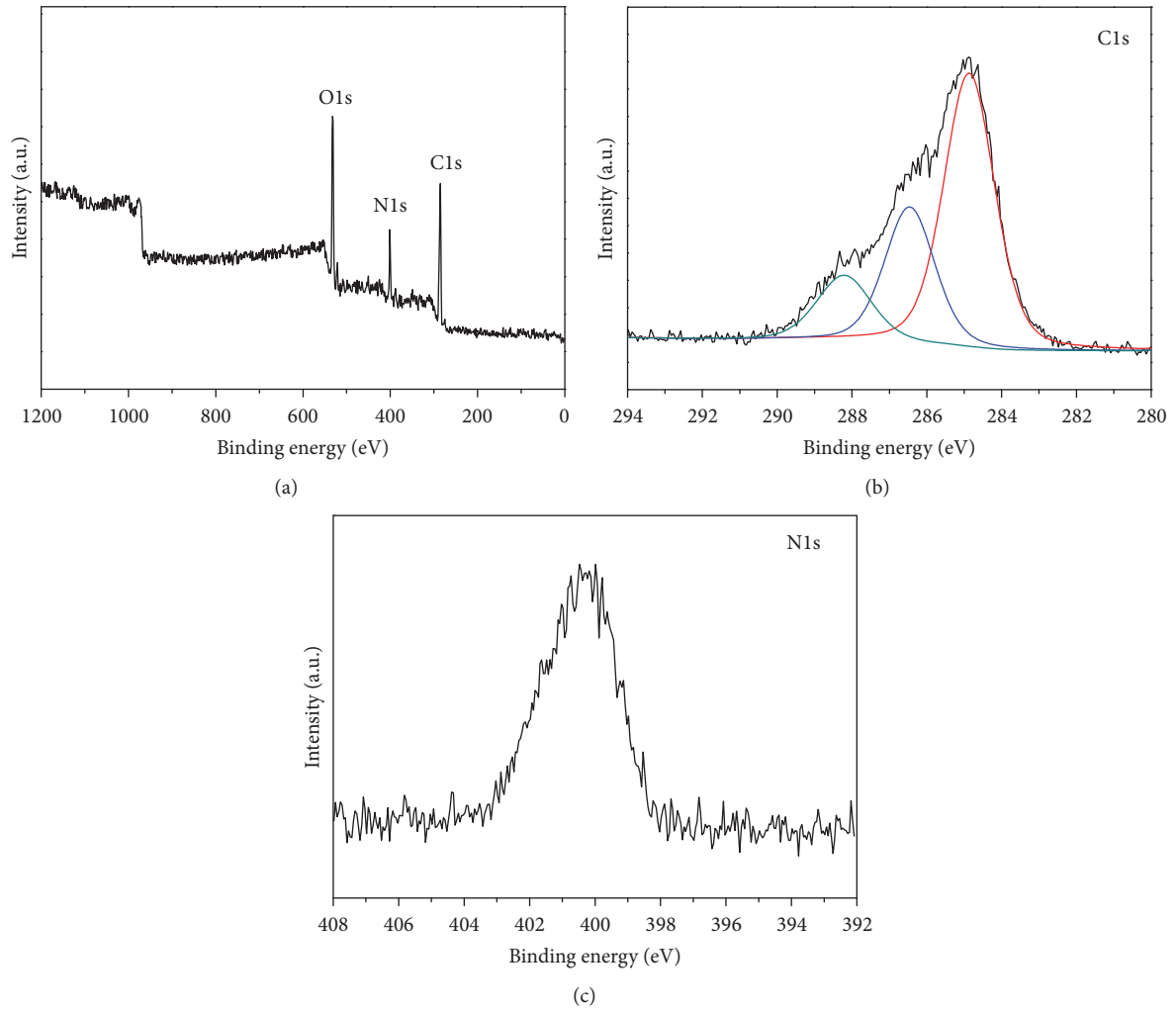

Figure 4: (a) Full-scale XPS spectrum of N-GQDs prepared by citric acid: ethylenediamine=1:3; (b) high resolution XPS spectra of C1s; (c) high resolution XPS spectra of N1s.

Table 1: Elemental analysis table of N-GQDs prepared by different ethylenediamine content.

CA:EDA	N(%)	C(%)	H(%)	O(%)
1:1	13.9	33.1	7.9	45.1
1:2	14.1	34.8	8.1	43.0
1:3	15.1	36.2	8.5	40.2

N, and H elements, which indirectly indicates that the ratio of 1:3 makes CA and EDA fully reflect, forming more alkyl and amide groups. The fluorescence quantum yield of N-GQDs prepared by the ratio of 1:3 (CA and EDA) is up to 88.9%. Above analysis shows that N-GQDs contain amide groups, which can form intermolecular hydrogen bonds with water molecules and improve the water solubility of carbon quantum dots. Therefore, the as-prepared N-GQDs are well dispersed in water-ethanol blend solution.

3.1.2. Fluorescence Properties of N-GQDs. In order to investigate the effects of different ethylenediamine content, reaction time, and reaction temperature on the optical properties of N-GQDs, the ultraviolet absorption spectra and fluorescence spectra of the products under three reaction conditions were measured. As shown in Figure 5, Figure (a) shows the UV-Vis absorption spectra of graphene quantum dots prepared with different ethylenediamine contents. It can be seen from Figure 5 that the absorption peaks of carbon quantum dot solutions in the UV-Vis spectra at 260nm and 350nm at different reaction times are obvious. The absorption peaks at 260nm are mainly due to the π-$\pi*$ transition of C=C double bond, and the absorption peaks at 350nm are due to the transition of n-$\pi*$ of C=O double bond [37, 38]. These two absorption peaks also prove that there are certain absorption peaks in carbon quantum dots. The conjugate structure: by comparing the UV curves of different reaction time, it is found that the absorption intensity increases first

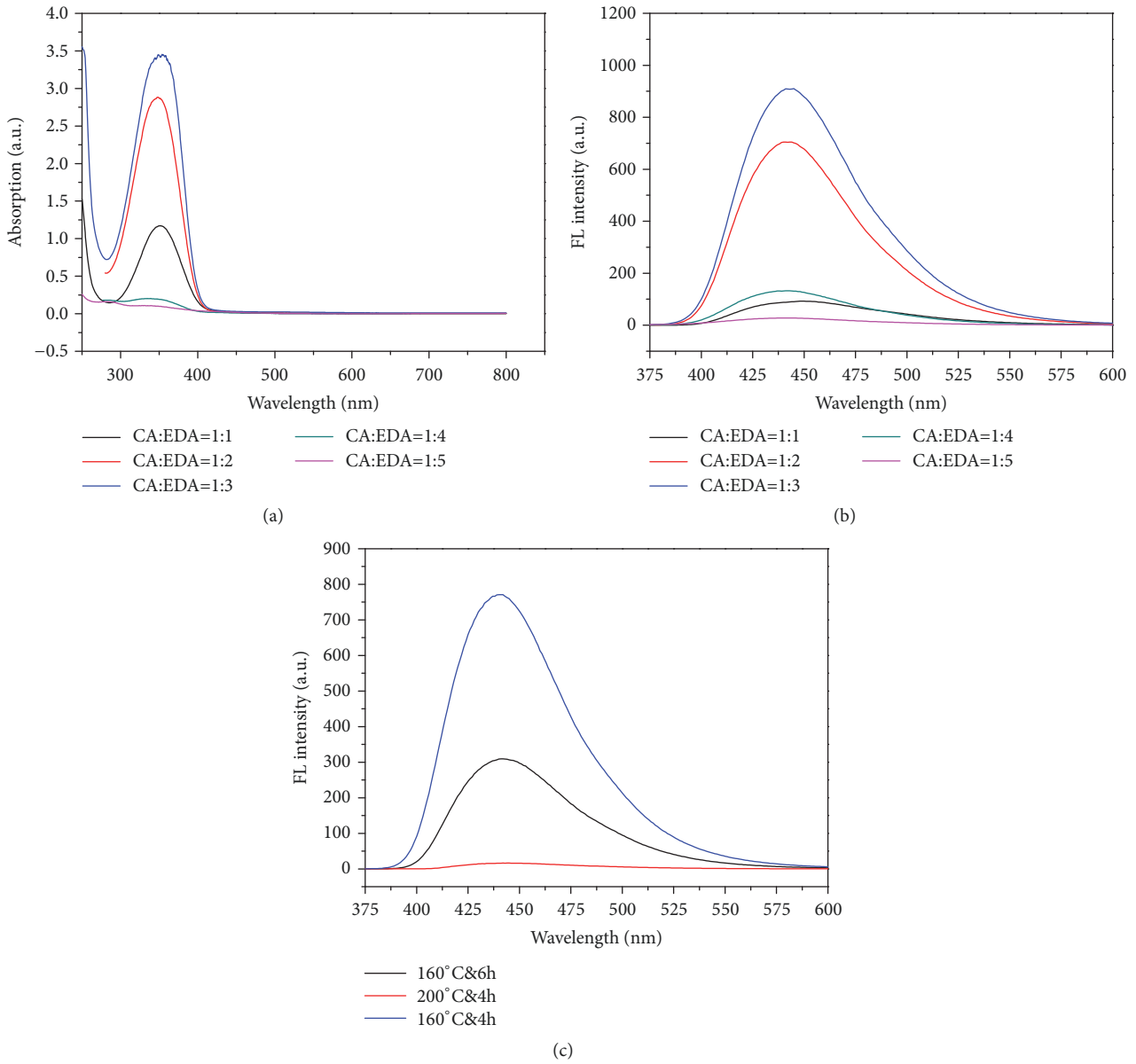

Figure 5: (a) UV-Vis absorption spectra of N-GQDs with different ethylenediamine content (the ratio of citric acid to ethylenediamine was 1:1, 1:2, 1:3, 1:4, and 1:5, respectively); (b) fluorescence intensity spectra of N-GQDs with different ethylenediamine content at 350nm excitation wavelength (the ratio of citric acid to ethylenediamine was 1:1, 1:2, 1:3, 1:4, and 1:5, respectively); (c) fluorescence intensity spectra at 350nm with different heating temperature and time.

and then decreases with the increase of ethylenediamine content, which indicates that the morphology, size, and quantity of carbon quantum dots will directly affect their optical properties. Figure 6(b) is the fluorescence emission spectrum of N-GQDs solution under 350nm excitation. It can be found that the fluorescence intensity of N-GQDs increases first and then decreases with the increase of ethylenediamine content. When the content of ethylenediamine increases, the reaction proceeds sufficiently, but once the reaction time exceeds the complete time, carbonization will occur, and because the distance between carbon quantum dots is small, reunion will occur with the increase of time, which will affect the fluorescence emission intensity. Figure 5(c) is the fluorescence emission spectrum of carbon quantum dot solution under 350nm excitation. It can be found that the fluorescence intensity of N-GQDs increases first and then decreases with the increase of reaction temperature and time.

As shown in Figure 6, the blue fluorescence emission is independent of the excitation wavelengths. Besides, it is quite stable in a neutral solution. Based on the above results, the N-GQDs particles with uniform size and good dispersibility in aqueous solution can be obtained by mixing citric acid: ethylenediamine at 1:3 molar ratio and heating at 160°C for 4h. Under the excitation wavelength of 350nm (maximum absorption peak of ultraviolet-visible spectrum),

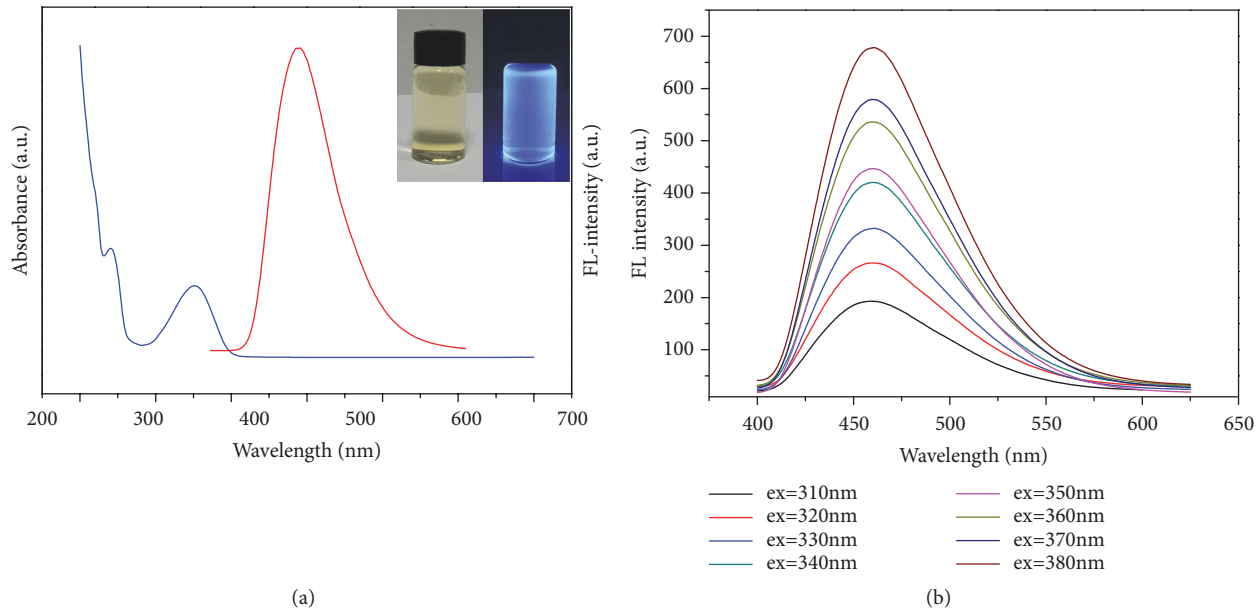

Figure 6: (a) UV-Vis absorbance and florescence spectra of N-GQDs in aqueous solution (CA:EDA=1:3); (b) photoluminescence of N-GQDs at different excitation wavelengths.

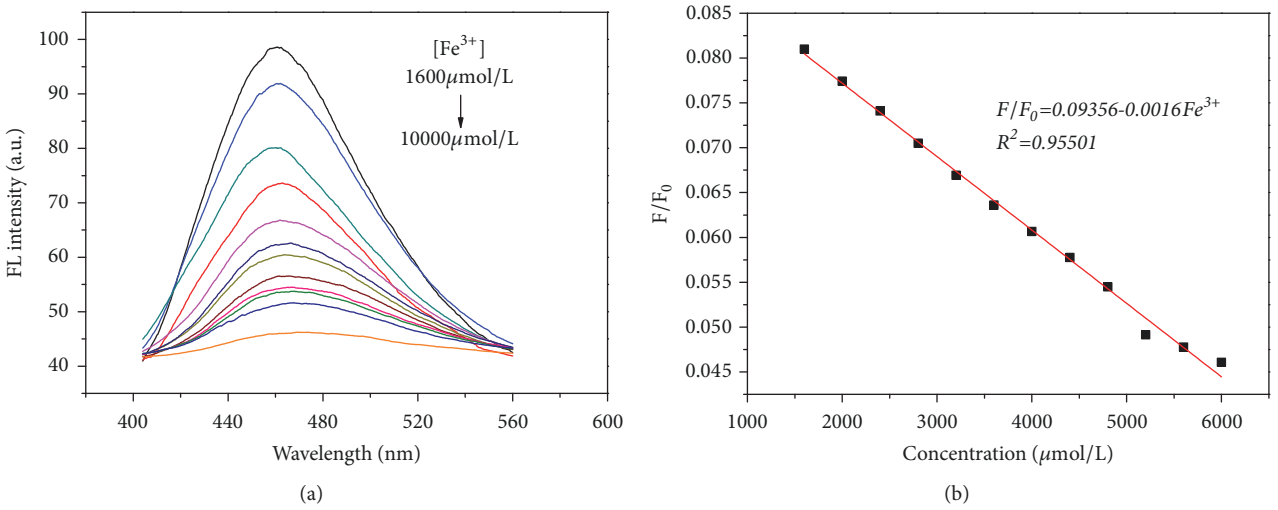

Figure 7: (a) Fluorescence spectra of iron ions with a concentration of 1600~10000μmol/L in the sample; (b) linear detection range of iron ions (the concentration of Fe^{3+} is1600~6000μmol/L).

the N-GQDs aqueous solution emits 456nm strong blue fluorescence.

3.2. Detection of Fe^{3+} by N-GQDs Probe Solution. In order to determine the detection ability of N-GQDs for Fe^{3+}, different concentrations of Fe^{3+} (1600~10000μmol/L) were added to 2g/L diluted by PBS to neutral N-GQDs solution, and the fluorescence spectra at 350nm excitation wavelength were determined as linear regression as shown in Figure 7. The N equation: the results show that the fluorescence intensity of N-GQDs solution is the highest when Fe^{3+} does not exist, and the peak value is 456nm. As shown in Figure 7(a), the fluorescence of N-GQDs at 456nm decreases with the increase of Fe^{3+} concentration. When the concentration of Fe^{3+} reaches 1600μmol/L, the fluorescence intensity begins to weaken linearly. When the concentration of Fe^{3+} reaches 10000μmol/L, the fluorescence of the solution almost disappears, indicating that N-GQDs are basically quenched. In Figure 7(b), scattering maps of N-GQDs fluorescence at 456nm at different Fe^{3+} concentrations are plotted. The results show that the fluorescence intensity of N-GQDs has a good linear relationship with the concentration of Fe^{3+} in the range of 1600~ 6000μmol/L mmol/L. The red solid line in the figure is a linear fitting curve, and the linear equation is (F/F_0=0.09356-0.00164Fe^{3+}, R^2=0.99501), in which F/F_0 is the ratio between the fluorescence intensity

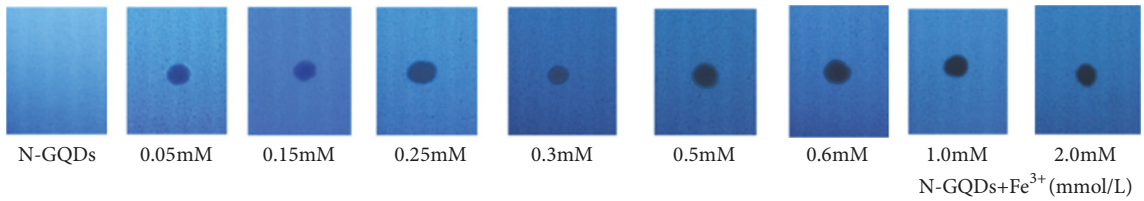

Figure 8: Titration of 0-2.0 mmol/L Ferric Ions in N-GQDs solutions (the concentration range of iron ions is 0-2.0mmol/L).

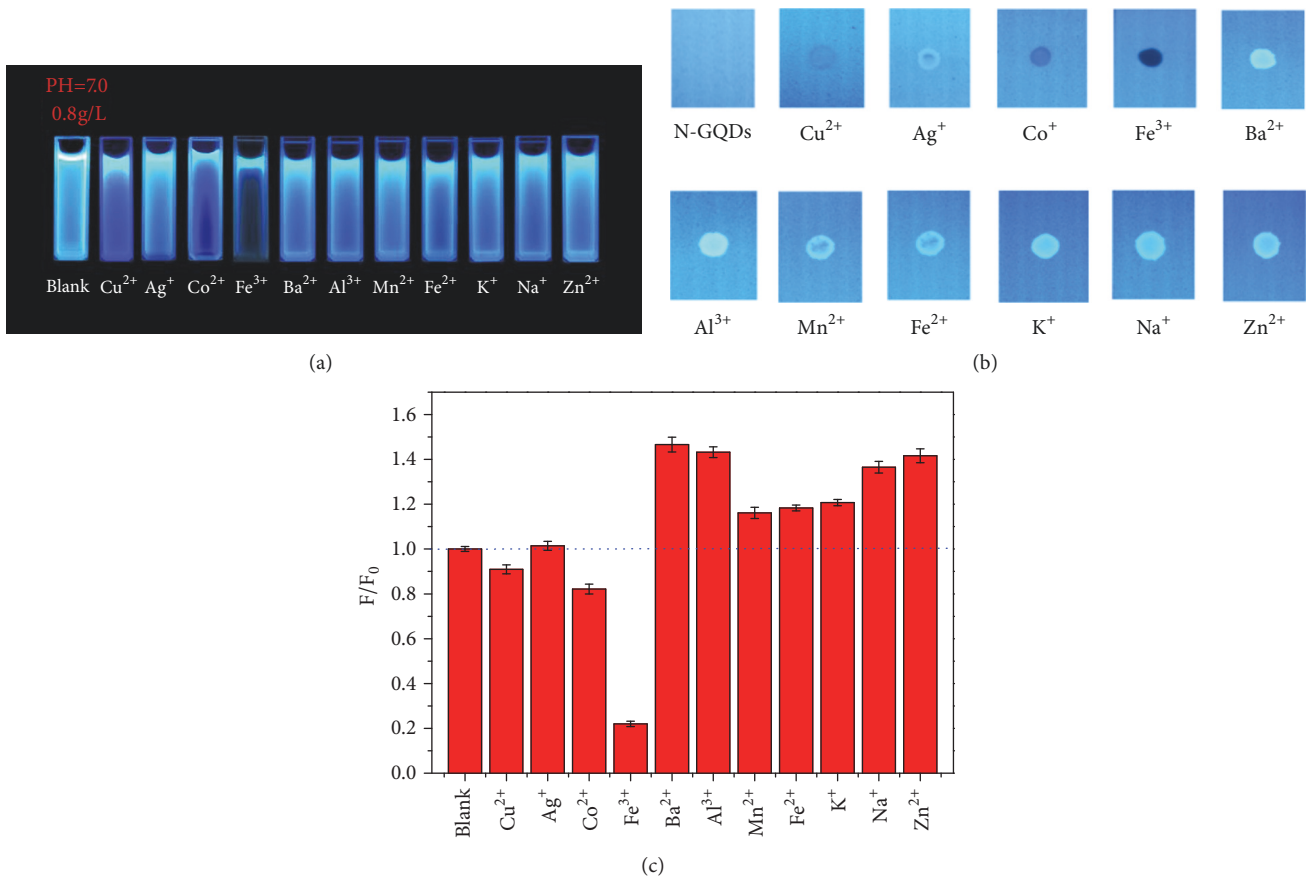

Figure 9: (a) Fluorescence probe solution with different metal ions irradiated by 365nm Ultraviolet Lamp; (b) drop coating of different metal ions on paper-based sensors; (c) fluorescence changes of N-GQDs in the presence of different metal ions (including Cu^{2+}, Ag^{+}, Co^{2+}, Fe^{3+}, Ba^{2+}, Al^{3+}, Mn^{2+}, Fe^{2+}, K^{+}, Na^{+}, and Zn^{2+} ions).

of probe and the initial fluorescence intensity of N-GQDs. The fluorescence intensity of the probe solution can be obtained by fitting. The detection limit is 2.37μmol/L, which meets the European Union (EC) requirement that the maximum permissible concentration of Fe^{3+} in drinking water is 3.57μmol/L.

3.3. Fluorescence Quenching Paper-Based Sensor for Visual Detection of Fe^{3+}. As shown in Figure 8, the fluorescence of test paper can be changed from strong to weak by different concentration of Fe^{3+}. When the concentration of Fe^{3+} reaches 0.5mmol/L, there is almost no fluorescence on paper base. When the concentration is higher, the fluorescence of fluorescent paper base is almost completely quenched, thus realizing the visual detection of Fe^{3+}.

3.3.1. Selectivity of Probe Solution. Photo and fluorescence spectra of N-GQDs after adding metal ions are shown in Figure 9. F_0 represents the fluorescence intensity of blank N-GQDs, and F represents the fluorescence intensity after adding metal ions. Photographs and spectrograms show that Fe^{3+} can quench N-GQDs violently, followed by Co^{2} also has an obvious quenching effect and Cu^{2+} has a slight quenching effect. When these ions coexist with Fe^{3+}, the effect of elimination is considered. The other metal ions have little effect on N-GQDs. The results show that the N-GQDs fluorescent probe can selectively identify Fe^{3+} ions.

As shown in Figure 9, it is observed that the fluorescence quenching of paper-based sensor is obvious when Fe^{3+} is added, while the quenching effect of other metal ions is not obvious. It shows that the fluorescence quenching type

paper-based sensor has good selectivity for the detection of Fe^{3+}.

4. Conclusion

In summary, we have successfully synthesized a kind of N-GQDs using CA and EDA as carbon and nitrogen sources by one-pot hydrothermal method. The N-GQDs have a strong blue fluorescence at 160°C for 4 hours. The QY of the N-GQDs is as high as 88.9%. Fluorescence emission is independent of excitation wavelength. In addition, these as-prepared N-GQDs can be well dispersed in water and ethanol solvents. The fluorescent probe based on N-GQDs solution has good recognition and sensitivity for Fe^{3+} with a linear range of 1600~6000μmol/L and a detection limit of 2.37μmol/L. In addition, fluorescence quenching paper-based sensors are constructed by immobilizing N-GQDs solution on paper-based, which achieves the visual detection of Fe^{3+}. Furthermore, the lowest concentration observed by naked eyes is 10000μmol/L, and much better selectivity has been obtained. It is believed that paper-based sensors based on N-GQDs will be more widely applied in visual fluorescence detection, which will make the detection of substances more efficient, environmentally friendly, and economical.

Data Availability

The data used to support the findings of this study are included within the article.

Conflicts of Interest

The authors declare that there are no conflicts of interest regarding the publication of this paper.

Acknowledgments

The authors gratefully recognize the financial support from the Hubei Natural Science Foundation (2017CFC888).

References

[1] Y. Wang and A. Hu, "Carbon quantum dots: synthesis, properties and applications," *Journal of Materials Chemistry*, vol. 2, no. 34, pp. 6921–6939, 2014.

[2] W. J. Lu, X. J. Gong, Z. H. Yang et al., "High-quality water-soluble luminescent carbon dots for multicolor patterning, sensors, and bioimaging," *RSC Advances*, vol. 5, no. 22, pp. 16972–16979, 2015.

[3] H. Ding, J.-S. Wei, and H.-M. Xiong, "Nitrogen and sulfur co-doped carbon dots with strong blue luminescence," *Nanoscale*, vol. 6, no. 22, pp. 13817–13823, 2014.

[4] J. Liu, S. Lu, Q. Tang et al., "One-step hydrothermal synthesis of photoluminescent carbon nanodots with selective antibacterial activity against Porphyromonas gingivalis," *Nanoscale*, vol. 9, no. 21, pp. 7135–7142, 2017.

[5] R. Atchudan, T. N. J. I. Edison, K. R. Aseer, S. Perumal, N. Karthik, and Y. R. Lee, "Highly fluorescent nitrogen-doped carbon dots derived from Phyllanthus acidus utilized as a fluorescent probe for label-free selective detection of Fe^{3+} ions, live cell imaging and fluorescent ink," *Biosensors and Bioelectronics*, vol. 99, pp. 303–311, 2018.

[6] D. Qu, M. Zheng, L. Zhang et al., "Corrigendum: Formation mechanism and optimization of highly luminescent N-doped graphene quantum dots," *Scientific Reports*, vol. 4, no. 9, article 5294, 2014.

[7] Y. Li, Y. Hu, Y. Zhao et al., "An electrochemical avenue to green-luminescent graphene quantum dots as potential electron-acceptors for photovoltaics," *Advanced Materials*, vol. 23, no. 6, pp. 776–780, 2011.

[8] B. Y. Fang, C. Li, Y. Y. Song et al., "Nitrogen-doped graphene quantum dot for direct fluorescence detection of Al^{3+}, in aqueous media and living cells," *Biosensors and Bioelectronics*, 2017, S0956566317305894.

[9] H. Tetsuka and T. Matsui, "Non-ionic fluorosurfactant improves wettability of nitrogen-functionalized graphene quantum dots for integration with optoelectronic devices," *Chemistry Letters*, vol. 47, no. 7, pp. 850–852, 2018.

[10] H. Tetsuka, A. Nagoya, T. Fukusumi et al., "Molecularly designed, nitrogen-functionalized graphene quantum dots for optoelectronic devices," *Advanced Materials*, vol. 28, no. 23, pp. 4755-4755, 2016.

[11] B. Bali Prasad, A. Kumar, and R. Singh, "Synthesis of novel monomeric graphene quantum dots and corresponding nanocomposite with molecularly imprinted polymer for electrochemical detection of an anticancerous ifosfamide drug," *Biosensors and Bioelectronics*, vol. 94, pp. 1–9, 2017.

[12] C. Fan, K. Ao, P. Lv et al., "Fluorescent Nitrogen-Doped Carbon Dots, via, Single-Step Synthesis Applied as Fluorescent Probe for the Detection of Fe^{3+}, Ions and Anti-Counterfeiting Inks," *NANO*, vol. 13, no. 08, 2018.

[13] J. Gu, X. Zhang, A. Pang et al., "Facile synthesis and photoluminescence characteristics of blue-emitting nitrogen-doped graphene quantum dots," *Nanotechnology*, vol. 27, article 165704, no. 16, 2016.

[14] H. Safardoust-Hojaghan, M. Salavati-Niasari, O. Amiri et al., "Preparation of highly luminescent nitrogen doped graphene quantum dots and their application as a probe for detection of Staphylococcus aureus, and E. coli," *Journal of Molecular Liquids*, vol. 241, 2017.

[15] B. Wang, S. Zhuo, L. Chen, and Y. Zhang, "Fluorescent graphene quantum dot nanoprobes for the sensitive and selective detection of mercury ions," *Spectrochimica Acta Part A: Molecular and Biomolecular Spectroscopy*, vol. 131, pp. 384–387, 2014.

[16] Y. Wang, S. Zhao, M. Li et al., "Graphene quantum dots decorated graphene as an enhanced sensing platform for sensitive and selective detection of copper(II)," *Journal of Electroanalytical Chemistry*, vol. 797, pp. 113–120, 2017.

[17] L. Jin, Y. Wang, F. Liu, S. Yu, Y. Gao, and J. Zhang, "The determination of nitrite by a graphene quantum dot fluorescence quenching method without sample pretreatment," *Luminescence*, vol. 33, no. 2, pp. 289–296, 2017.

[18] L. Lin, M. Rong, S. Lu et al., "A facile synthesis of highly luminescent nitrogen-doped graphene quantum dots for the detection of 2,4,6-trinitrophenol in aqueous solution," *Nanoscale*, vol. 7, no. 5, pp. 1872–1878, 2015.

[19] Q. Xu, P. Pu, J. Zhao et al., "Preparation of highly photoluminescent sulfur-doped carbon dots for Fe(iii) detection," *Journal of Materials Chemistry A*, vol. 3, no. 2, pp. 542–546, 2015.

[20] L. Tang, R. Ji, X. Li, K. S. Teng, and S. P. Lau, "Energy-level structure of nitrogen-doped graphene quantum dots," *Journal of Materials Chemistry C*, vol. 1, no. 32, pp. 4908–4915, 2013.

[21] Y. Li, Y. Zhao, H. Cheng et al., "Nitrogen-doped graphene quantum dots with oxygen-rich functional groups," *Journal of the American Chemical Society*, vol. 134, no. 1, pp. 15–18, 2012.

[22] J. Ju and W. Chen, "Synthesis of highly fluorescent nitrogen-doped graphene quantum dots for sensitive, label-free detection of Fe (III) in aqueous media," *Biosensors and Bioelectronics*, vol. 58, pp. 219–225, 2014.

[23] S. J. Zhu, Q. N. Meng, L. H. Wang et al., "Highly photoluminescent carbon dots for multicolor patterning, sensors, and bioimaging," *Angewandte Chemie International Edition*, vol. 52, no. 14, pp. 3953–3957, 2013.

[24] S. Zhu, Y. Song, J. Shao et al., "Non-conjugated polymer dots with crosslink-enhanced emission in the absence of fluorophore units," *Angewandte Chemie*, vol. 47, no. 6, pp. 14626–14637, 2016.

[25] C. Xia, S. Tao, S. Zhu et al., "Hydrothermal addition polymerization for ultrahigh-yield carbonized polymer dots with room temperature phosphorescence via nanocomposite," *Chemistry - A European Journal*, vol. 24, no. 44, pp. 11303–11308, 2018.

[26] Y. Han, D. Tang, Y. Yang et al., "Non-metal single/dual doped carbon quantum dots: a general flame synthetic method and electro-catalytic properties," *Nanoscale*, vol. 7, no. 14, pp. 5955–5962, 2015.

[27] S. Bak, D. Kim, and H. Lee, "Graphene quantum dots and their possible energy applications: a review," *Current Applied Physics*, vol. 16, no. 9, pp. 1192–1201, 2016.

[28] A. Madni, S. Noreen, I. Maqbool et al., "Graphene based nanocomposites: synthesis and their theranostic applications," *Journal of Drug Targeting*, pp. 1–69, 2018.

[29] M. Bahram, K. Farhadi, and F. Arjmand, "Voltammetric determination of dopamine in the presence of ascorbic and uric acids using partial least squares regression: determination of dopamine in human urine and plasma," *Open Chemistry*, vol. 7, no. 3, pp. 524–531, 2009.

[30] D. Qu, M. Zheng, J. Li et al., "Tailoring color emissions from N-doped graphene quantum dots for bioimaging applications," *Light: Science & Applications*, vol. 4, no. 12, p. e364, 2015.

[31] D. Qu, M. Zheng, P. Du et al., "Highly luminescent S, N co-doped graphene quantum dots with broad visible absorption bands for visible light photocatalysts," *Nanoscale*, vol. 5, no. 24, pp. 12272–12277, 2013.

[32] D. Qu, M. Zheng, L. Zhang et al., "Formation mechanism and optimization of highly luminescent N-doped graphene quantum dots," *Scientific Reports*, vol. 4, 2014.

[33] X. Fan, B. D. Phebus, L. Li, and S. Chen, "Chemical functionalization of graphene quantum dots," *Science of Advanced Materials*, vol. 7, no. 10, pp. 1990–2010, 2015.

[34] A. Karimzadeh, M. Hasanzadeh, N. Shadjou et al., "Electrochemical biosensing using N-GQDs: Recent advances in analytical approach," *TrAC - Trends in Analytical Chemistry*, vol. 105, pp. 484–491, 2018.

[35] J. Soleymani, M. Hasanzadeh, M. H. Somi, S. A. Ozkan, and A. Jouyban, "Targeting and sensing of some cancer cells using folate bioreceptor functionalized nitrogen-doped graphene quantum dots," *International Journal of Biological Macromolecules*, vol. 118, pp. 1021–1034, 2018.

[36] Z. Li, H. Yu, T. Bian et al., "Highly luminescent nitrogen-doped carbon quantum dots as effective fluorescent probes for mercuric and iodide ions," *Journal of Materials Chemistry C*, vol. 3, no. 9, pp. 1922–1928, 2015.

[37] S. Dhar, T. Majumder, and S. P. Mondal, "Phenomenal improvement of external quantum efficiency, detectivity and responsivity of nitrogen doped graphene quantum dot decorated zinc oxide nanorod/polymer schottky junction UV detector," *Materials Research Bulletin*, vol. 95, pp. 198–203, 2017.

[38] A. Karimzadeh, M. Hasanzadeh, N. Shadjou, and M. D. L. Guardia, "Electrochemical biosensing using N-GQDs: Recent advances in analytical approach," *TrAC - Trends in Analytical Chemistry*, vol. 105, pp. 484–491, 2018.